FEBS Letters 584 (2010) 493–499

FEBS Letters

journal homepage: www.FEBSLetters.org

Myosin 1G (Myo1G) is a haematopoietic specific myosin that localises to the plasma membrane and regulates cell elasticity

Balaji Olety [a], Mike Wälte [b], Ulrike Honnert [a], Hermann Schillers [b], Martin Bähler [a,*]

[a] Institute of General Zoology and Genetics, Westfalian Wilhelms-University Münster, Germany
[b] Institute of Physiology II, Westfalian Wilhelms-University Münster, Germany

ARTICLE INFO

Article history:
Received 3 September 2009
Revised 10 November 2009
Accepted 30 November 2009
Available online 4 December 2009

Edited by Berend Wieringa

Keywords:
Myo1G
Myosin
Actin
Cell elasticity
Haematopoietic
PH-domain

ABSTRACT

Immune cells navigate through different environments where they experience different mechanical forces. Responses to external forces are determined by the mechanical properties of a cell and they depend to a large extent on the actin-rich cell cortex. We report here that Myo1G, a previously uncharacterised member of class I myosins, is expressed specifically in haematopoietic tissues and cells. It is associated with the plasma membrane. This association is dependent on a conserved PH-domain-like myosin I tail homology motif and the head domain. However, the head domain does not need to be a functional motor. Knockdown of Myo1G in Jurkat cells decreased cell elasticity significantly. We propose that Myo1G regulates cell elasticity by deformations of the actin network at the cell cortex.

Structured summary:
MINT-7307273: *MYO1G* (uniprotkb:B0I1T2) and *Actin* (uniprotkb:P60709) *colocalize* (MI:0403) by *fluorescence microscopy* (MI:0416)
MINT-7307283: *TfR* (uniprotkb:P02786) and *MYO1G* (uniprotkb:B0I1T2) *colocalize* (MI:0403) by *cosedimentation through density gradients* (MI:0029)

1. Introduction

Class I myosins are single-headed actin-based motor molecules that are widely expressed. Myo1G, one of eight class I members expressed in mammals (Myo1a–Myo1h), has been found in cholesterol-rich detergent resistant membrane fragments from neutrophils and to be enriched in fractions of membrane and microvilli from peripheral blood T-lymphocytes and a mouse pre-B lymphocyte cell line [1,2]. Based on sequence homology, Myo1G forms a subclass together with Myo1d (named previously myr 4). Class I myosins consist of a N-terminal motor domain, a myosin light chain binding domain with variable numbers of IQ-motifs, and a C-terminal tail domain. This tail domain is rich in basic residues and associates with membranes [3–7]. Class I myosins have been implicated in various cellular processes relying on actin-dependent membrane dynamics such as endocytosis, secretion, adhesion, motility and regulation of mechanosensitive channels [8]. Myo1d has been reported to regulate endocytic membrane trafficking along the recycling pathway in epithelial MDCK cells [9]. In *Drosophila melanogaster* the loss of Myo31DF, a Myo1d ortholog, causes a complete reversal of the left/right axis with the gut, testis and spermiduct looping sinistrally instead of dextrally [10,11].

Cells face not only a complex biochemical, but also a diverse biomechanical environment. They sense and respond to different mechanical forces and convert them into biochemical signals [12,13]. Nearly all cells in the body are continuously stretched and squeezed. In particular immune cells such as T-cells that patrol between different organs and tissues are exposed to different mechanical forces. The mechanical properties such as cell elasticity are hence important for cell function. Elasticity of cells is determined to a large extent by the actin cytoskeleton. Myosins might control internal tension and hence the elasticity of cells. Indeed, the simultaneous loss of multiple class I myosins in the slime mold *Dictyostelium discoideum* resulted in a decrease of cortical tension, whereas overexpression of class I myosins increased cortical tension [14]. Mouse enterocytes that do not express Myo1A exhibited a reduced membrane tension and conversely the overexpression of several mammalian class I myosins increased membrane tension [15].

We report here the initial characterization of Myo1G, a class I myosin expressed specifically in the haematopoietic system. It associates with the plasma membrane through a PH-like domain and contributes to the elasticity of Jurkat T-cells.

* Corresponding author. Address: Institut für Allgemeine Zoologie und Genetik, Westfälische Wilhelms Universität, Schlossplatz 5, 48149 Münster, Germany. Fax: +49 251 83 24723.
E-mail address: baehler@uni-muenster.de (M. Bähler).

0014-5793/$36.00 © 2009 Federation of European Biochemical Societies. Published by Elsevier B.V. All rights reserved.
doi:10.1016/j.febslet.2009.11.096

2. Materials and methods

2.1. Cell culture and transfections

B16-F1 mouse melanoma (ATCC CRL-6323) and Jurkat (ATCC TIB-152) cells were cultured in high glucose DMEM (PAA, Germany) and RPMI-1640 (ATCC Cat No. 30-2001), respectively, supplemented with 10% heat inactivated fetal calf serum, 2 mM L-glutamine (Invitrogen, Karlsruhe, Germany), 50 U/ml penicillin (Invitrogen), and 0.05 mg/ml streptomycin (Invitrogen). They were incubated at 37 °C in a humidified atmosphere with 5% CO_2. B16-F1 cells were cultured on 60-mm diameter dishes to 60% confluence and transfected by using SuperFect reagent (QIAGEN, Hilden, Germany) as instructed by the manufacturer.

2.2. Subcellular fractionation and tissue preparation

Jurkat cells were harvested in PBS and centrifuged at 100×*g* for 10 min. Pelleted cells were resuspended in ice-cold hypotonic buffer (10 mM KCl, 2 mM $MgCl_2$, 5 mM HEPES, pH 7.4) and incubated for 15 min on ice. The cell suspension was then passed through a 26G needle for 20 times. The lysed cells were centrifuged at 500×*g* for 10 min at 4 °C to separate the PNS (post nuclear supernatant) and nuclear pellet fractions. The PNS was collected and mixed with a 66% (w/w) sucrose solution before it was carefully layered at the bottom of a pre-made 25–55% (w/w) continuous sucrose gradient. The gradient was centrifuged in a Beckmann ultracentrifuge SW-41 rotor at 22,000 rpm and 4 °C for 22 h. Fractions were collected starting from the bottom of the tube. Equal volumes of the fractions were then resolved by 7.5% SDS–PAGE, transferred to PVDF membrane and probed for Myo1G and transferrin receptor.

Different mouse tissues were homogenised by a dounce homogeniser in homogenisation buffer (0.32 M sucrose, 15 mM HEPES, pH 7.4) and the protein concentration was determined by the method of Bradford. Equal amounts of proteins were then resolved by 7.5% SDS–PAGE and probed for Myo1G.

2.3. Plasmid constructs and antibodies

Myo1G cDNA was synthesized by RT-PCR from total RNA isolated from mouse spleen. Constructs encompassing different regions of Myo1G, namely full length Myo1G, IQ+tail (aa 718–1024), tail (aa 762–1024) and tail homology motif (aa 824–938) were cloned in to pEGFP-C1 vector between *BglII* and *SalI* sites. The mutations in the head domain (G111R, R167C) and the 'PH-like' domain (K883A, R893A) were introduced by Quick-change Site-Directed Mutagenesis (Stratagene) and confirmed by sequencing. Antibodies against Myo1G were raised against a synthetic peptide (aa 7–19, MEDEEGPEYGKPDC) in a rabbit (758). Alternatively, Myo 1G antibodies were purchased from Rockland (cat no. 600-401-959). Transferrin receptor antibody was from cymbus biotechnology Ltd. (Cat no. CBL137B). Antibodies against Myo 1B (Tü 23) were raised against the fusion protein encoding amino acids 590–690 of rat Myo1B. Myo 1C (Tü 45) antibodies were raised against a synthetic peptide (FVLHVQREDSKQKGDC). Myo 1D (SA482) [9] and Myo1E (Tü 58) [16] antibodies have been described previously.

2.4. Silencing of Myo1G in Jurkat cells

For silencing of Myo1G expression, Jurkat cells were transfected with 8 µl of 20 µM stock On-Target plus SMART pool siRNA (cat# L-025326-01, Dharmacon) using the Amaxa Nucleofector II system specific for Jurkat cells. On-target plus non-targeting pool siRNA were used as controls (catalog #D-001810-01-05, Dharmacon). The siRNA mediated Myo1G knockdown was verified by western blot at 72 h post-transfection and quantified by ImageJ. The transfection efficiency of Jurkat cells by siRNA was determined with FACS using FITC-labelled siRNA. The siRNAs targeting human MYO1G used in this study were as follows: 5′-CUGUUUGCUCAGCGACUAA-3′, 5′-GCACCAUCACUGACCGAAU-3′, 5′-CGUCAACAGUUUCGAGCAG-3′, 5′-GCAAUGAAGCACCGGUCCA-3′.

2.5. Immunofluorescence microscopy and image acquisition

B16-F1 cells were replated on sterile coverslips coated with mouse laminin (25 µg/ml, 1 h) 24 h after transfection and incubated for an additional 4 h before fixation. Jurkat cells were plated for 1 h on human fibronectin (10 µg/ml) coated glass cover slips before fixation and immunostaining. Cells were washed with PBS to remove unattached cells, fixed with 4% paraformaldehyde for 20 min and washed twice with PBS. They were then permeabilized with 0.1% Triton X-100 in PBS for 1 min and blocked with 2% BSA in PBS for 30 min to prevent nonspecific binding. Cells were incubated with primary antibodies in 1% BSA for 1 h at room temperature, followed by washing thrice with PBS and incubation with fluorescently labelled secondary antibodies in 1% BSA for 1 h at room temperature along with Texas red-phalloidin to stain actin filaments. The cells were washed thrice with PBS and mounted in mowiol. Jurkat cells were viewed using a confocal microscope (Zeiss LSM 510, 63X oil immersion, NA 1.4) whereas B16-F1 melanoma cells were viewed using an epifluorescence microscope

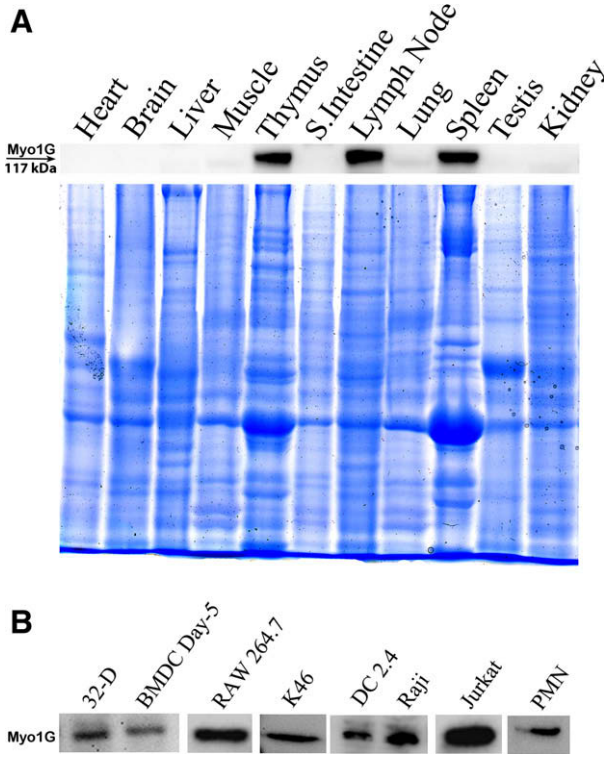

Fig. 1. Myo1G is expressed specifically in haematopoietic cells. Expression of Myo1G was analysed in different tissues and cell types by immunoblotting. Tissue and cell homogenates were prepared as described in Section 2. (A) Equal amounts of protein were loaded from each tissue homogenate and (B) from different cell lines and probed with Myo1G antibody. Equal protein loading of tissue homogenates was confirmed by staining a corresponding gel with Coomassie blue. Tissues and cell lines are indicated. 32-D, myeloblast like cell line; BMDC day-5, bone marrow derived dendritic cells cultured for 5 days in vitro; RAW 264.7, macrophage cell line; DC2.4, dendritic cell line; Raji, B-cell line; Jurkat, T cell line; PMN, mouse polymorphonuclear leucocytes.

(Zeiss Axiophot). Images were assembled in Adobe Photoshop (version CS2).

2.6. Force spectroscopy of Jurkat cells

Jurkat cells were plated on fibronectin coated coverslips (10 μg/ml) and briefly washed with PBS. Calibration, elasticity measurements and data processing were performed as described [17–19] using a Nanoscope III Multimode-AFM (Veeco Instruments, Santa Barbara, California, USA). All measurements were carried out in a fluid cell at 37 °C (MMFHTR-2 Air and Fluid Sample Heater, Veeco Instruments). Colloidal probes with a sphere radius of 0.5 μm were used for this work (PT.PS, Novascan Technologies, Armes, IA, USA). Probes were placed under optical control (OMV-PAL, Veeco Instruments) over the center of the cells and force–distance curves were obtained with a constant approach velocity of 1 μm/s. Each cell was indented once using a constant loading force of 2 nN. The force–distance curves were analysed 200 nm from the contact point of the cell to obtain Young's modulus (*E*).

3. Results

3.1. Myo1G is expressed specifically in haematopoietic tissues and cells

The expression patterns of class I myosin's differ greatly in multi-cellular organisms. To determine the tissue distribution of Myo1G, we used antibodies that specifically recognized EGFP-Myo1G in transfected B16-F1 melanoma cells (data not shown).

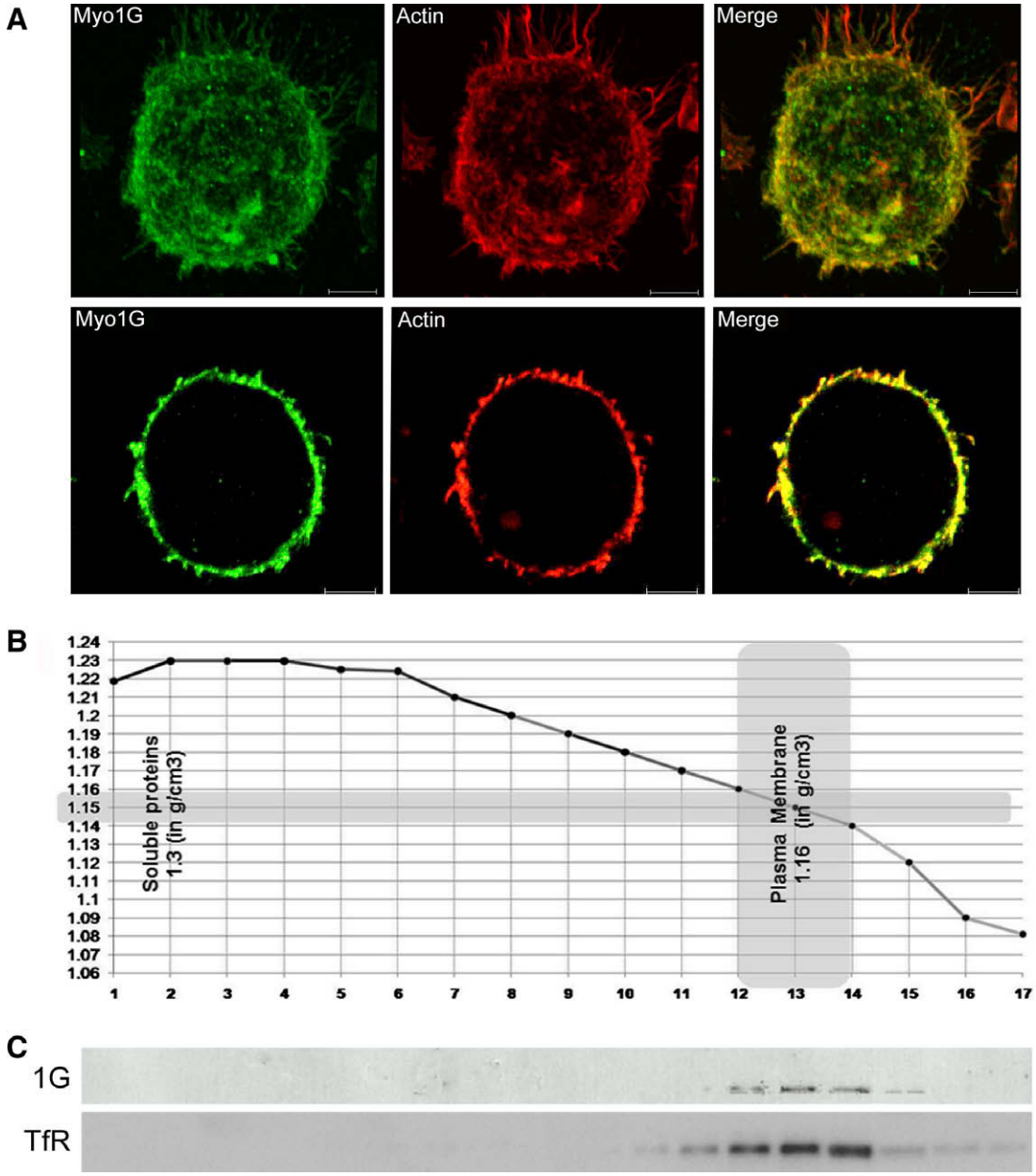

Fig. 2. Myo1G localizes to the plasma membrane. The subcellular localization of Myo1G in Jurkat cells was analysed by indirect immunofluorescence and subcellular fractionation as described in Section 2. (A) Myo1G was labelled using rabbit anti-Myo1G antibody and an AlexaFluor® 488 goat anti-rabbit secondary antibody. F-actin was labelled with TexasRed Phalloidin. Confocal composite images (top row) and confocal midplane sections (bottom row) are shown. Scale bar, 5 μm. The postnuclear supernatant of Jurkat cells was subjected to fractionation on a linear sucrose density gradient. The densities of different fractions were analysed by refractometry (B). The distribution of Myo 1G (1G) and transferrin receptor (TfR) was monitored by separating equal volumes of the collected fractions by SDS–PAGE and immunoblotting (C).

Myo1G was detected in adult tissues of the immune system such as thymus, lymph nodes and spleen, but not in brain, lung, heart, liver, small intestine, testis, and kidney (Fig. 1A). It was expressed in mouse PMN leucocytes, bone marrow derived dendritic cells and in several hematopoietic cell lines that were of macrophage, B-, T-, and dendritic cell origin (Fig. 1B).

3.2. Myo 1G is associated with the plasma membrane

As a first step towards establishing potential functions of Myo1G, we analysed its subcellular distribution in Jurkat cells (Fig. 2). Confocal fluorescence microscopy revealed that Myo1G was associated with the plasma membrane in Jurkat cells (Fig. 2A). The cell surface of Jurkat cells is covered by highly irregular cell protrusions as seen in a midplane confocal section leading to a speckled appearance of the fluorescence in composite confocal images. Subcellular fractionation of Jurkat cells confirmed the association of Myo1G with the plasma membrane. Fractions containing Myo1G exhibited a density of 1.14–1.16 g/cm^3 that corresponds to the density expected of the plasma membrane (1.16 g/cm^3) (Fig. 2B). Myo1G co-fractionated with the transferrin receptor (TfR) that served as a marker for the plasma membrane (Fig. 2C). Membranes derived from the endoplasmic reticulum fractionate in an overlapping, but not identical manner to the plasma membrane. Together, these results demonstrate that Myo1G localises to the plasma membrane.

3.3. Targeting of Myo1G to the plasma membrane

We next investigated how Myo1G is targeted to the plasma membrane. For that purpose we generated various mutated and truncated constructs of Myo1G and transiently transfected them into B16-F1 mouse melanoma cells. Although B16-F1 cells do not express detectable amounts of Myo1G, Myo1G fused either at the N- or C-terminus of EGFP localized to the plasma membrane (Fig. 3A and data not shown). A functional motor domain was not necessary for proper subcellular localization (Fig. 3B and C). Introduction of a point mutation in the nucleotide-binding P-loop (G111R; Myo1G^{G111R}) that is predicted to abolish nucleotide-binding [20] and block the chemo-mechanical cycling of Myo1G in the nucleotide-free state, did not change the localization in a significant manner (Fig. 3B). Similarly, a point mutation (R167C; Myo1G^{R167C}) predicted to abolish ATP hydrolysis [21,22] and block cycling in the ATP-bound state did not block targeting to the plasma membrane (Fig. 3C). Occasionally, the mutant Myo1GG111R exhibited a slightly increased cytosolic pool. These results indicated that a functional motor domain that cycles between different nucleotide-binding states is not necessary for Myo1G targeting to the plasma membrane, but may increase it somewhat. Overexpression of the mentioned constructs did not result in any obvious changes of the actin cytoskeleton (Fig. 3A′–C′).

It has been previously reported that class I short tailed myosin's have a PH-like domain characterised by a β1-loop-β2 motif in their

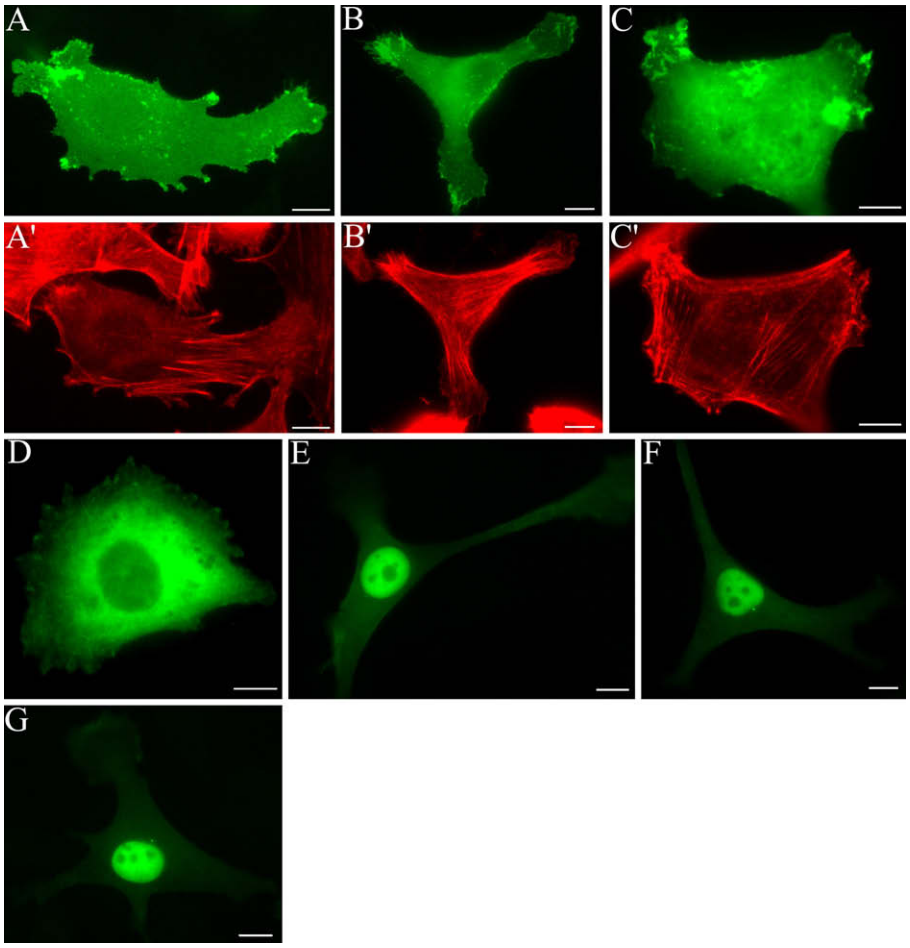

Fig. 3. Targeting of Myo1G to the plasma membrane of B16-F1 mouse melanoma cells. B16-F1 cells were transiently transfected with different EGFP-Myo1G constructs (green) and viewed in the fluorescence microscope. Some cells were simultaneously labelled for F-actin with TexasRed-phalloidin. (A, A′), EGFP-Myo1G; (B, B′), EGFP-Myo1G G111R; (C, C′), EGFP-Myo1G R167C. A–C EGFP fluorescence and A′–C′ corresponding F-actin stainings. (D) EGFP-Myo1G K883A-R893A; (E) EGFP-IQ+tail; (F) EGFP-tail; (G) EGFP-Myo1G tail homology motif (AA 824–938). Scale bars, 10 μm.

tail region [6]. For mammalian Myo1C this motif has been reported to bind to phosphoinositide-(4,5)-bis-phosphate on the plasma membrane [23]. To check if this is also the case for Myo1G, we mutated two conserved basic residues in the PH-like domain to alanine residues (K883A, R893A). These two point mutations abolished plasma membrane localization and redistributed Myo1G to the cytosol (Fig. 3D). Interestingly, we found that the motor domain of Myo1G is essential for proper localization. The truncated constructs IQ's+tail and tail localized preferentially to the nucleus and only a minor fraction localized to the plasma membrane (Fig. 3E and F). We have previously identified a conserved myosin I tail homology motif [24]. This motif encompasses the PH-like domain and spans in mouse Myo1G amino acids 824–938. Expression of this myosin I tail homology motif revealed that it localized in a similar manner as IQ+tail and tail. It was found in the nucleus and at the plasma membrane (Fig. 3G). Together these data indicate that both the PH-Like domain and the motor domain of Myo1G contribute to the subcellular targeting of Myo 1G in cells.

3.4. Knockdown of Myo1G decreases cell elasticity

Since Myo1G can interact with F-actin and is specifically localized at the plasma membrane, we asked if Myo1G affects cell elasticity. To test this, we depleted Jurkat cells of Myo1G by siRNA (Fig. 4A). Seventy two hours post nucleofection, the amount of Myo1G was reduced by 69%. Nucleofection of Jurkat cells with FITC-siRNA demonstrated that the majority of cells (89%) had taken up the siRNA (Fig. 4B). Class I myosins might act redundantly. Therefore, we investigated the expression of several other class I myosins in Jurkat cells that had been treated with Myo1G siRNA or non-targeting siRNA (Fig. 4A). We detected the expression of Myo1B splice variants, Myo1C and weakly of Myo1E, but not of Myo 1D, the closest relative of Myo 1G. No changes in their expression levels were observed in Jurkat cells that had been depleted of Myo 1G with siRNA. To determine the elasticity of adherent Jurkat cells, we measured the force–indentation relationship. We indented the cells with a spherical glass bead mounted to an AFM cantilever (Fig. 5). The force–indentation data were then processed to calculate elasticity [17] that is referred to as Young's Modulus (E) and is given in Pascals (Pa). Elasticity describes the tendency of an object to deform along an axis when opposing forces are applied along that axis. It is a property of the constituent material and does not depend on size, shape and boundary conditions. Jurkat cells depleted of Myo1G showed a significantly lower Young's modulus {$E = 483$ Pa ± 14 (SEM), $n = 104$} compared to the cells transfected with non-targeting siRNA {$E = 602$ Pa ± 27 (SEM), $n = 98$} (Fig. 5). Untransfected Jurkat cells exhibited a similar Young's modulus {$E = 600$ Pa ± 25 (SEM), $n = 110$} as those transfected with non-targeting siRNA. In summary, these results demonstrate that Myo1G contributes to cell elasticity in a non-redundant manner with other class I myosin's in Jurkat cells.

4. Discussion

The new findings of this study are that Myo1G is expressed specifically in haematopoietic cells, associates with the plasma membrane, both the tail homology motif and the head domain contribute to plasma membrane targeting, and depletion of Myo1G reduces cell elasticity.

Myo1G is expressed in various immune cells important for innate and adaptive immune responses. It is localized specifically at the plasma membrane and therefore, is likely to link the plasma membrane dynamically with actin filaments. An identical localization of recombinant Myo1G was also observed in cells that do not normally express Myo1G. This observation excludes the notion that there is a receptor specifically expressed in immune cells. Class I myosins have been reported to interact with anionic phospholipids [3,4,7,25] and mammalian Myo1c has been shown to interact with phosphoinositides in vivo [6]. The binding site was mapped to a putative PH-domain that is identical to a previously described myosin class I tail homology motif [24]. This putative PH-domain is also necessary for the binding of Myo1G to the plasma membrane. The mutation of two positively charged residues in this domain abolished plasma membrane localization of Myo1G. However, the putative PH-like domain is not sufficient for tight plasma membrane association. We found that the myosin head domain contributes significantly to plasma membrane localization. Interestingly, this does not need to be a head domain with a functional ATPase cycle. A point mutation expected to abrogate ATP-hydrolysis did not affect localization and a point mutation that blocks nucleotide-binding increased only slightly the cytosolic localization. The first mutation is expected to block the ATPase cycle in a nucleotide state exhibiting a weak affinity for F-actin whereas the second mutation is predicted to induce a nucleotide state with a strong affinity for F-actin. Therefore, the contribution of the head domain to plasma membrane association appears not to be strictly coupled with F-actin-binding. The head domain might serve a more structural role in plasma membrane association, such

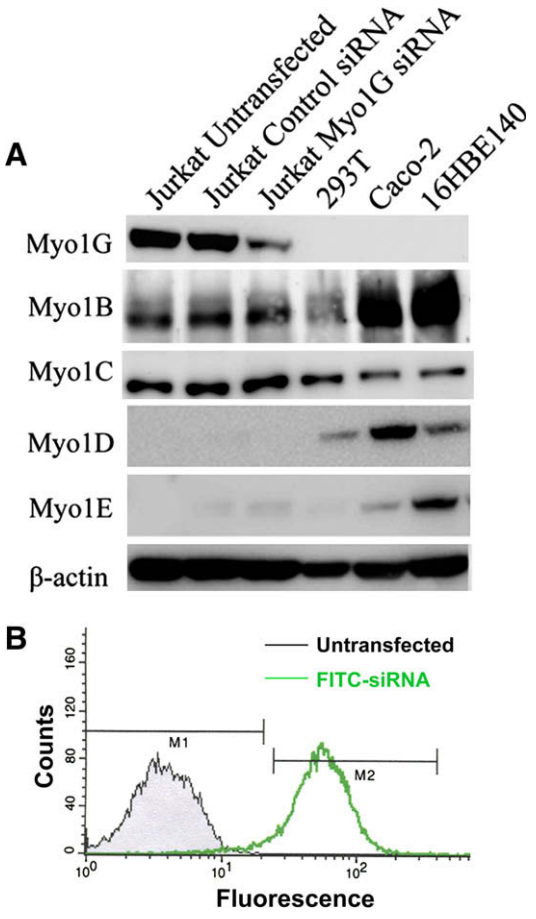

Fig. 4. Knockdown of Myo 1G and expression of other class I myosins in Jurkat cells. Jurkat cells were transfected either with control siRNA or siRNA's targeting different regions of Myo1G mRNA using nucleofection. Seventy two hours post transfection Jurkat cells were analysed. (A) Cell homogenates were subjected to immunoblotting to determine the levels of Myo1G depletion and the expression of Myo1B, Myo1C, Myo1D, Myo1E and β-actin. Homogenates of the cell lines 293T, Caco-2 and 16HBE14O were used as positive antibody controls. (B) Transfection efficiency was determined by transfecting Jurkat cells with FITC-labelled siRNA. Cellular uptake of FITC was analysed by FACS.

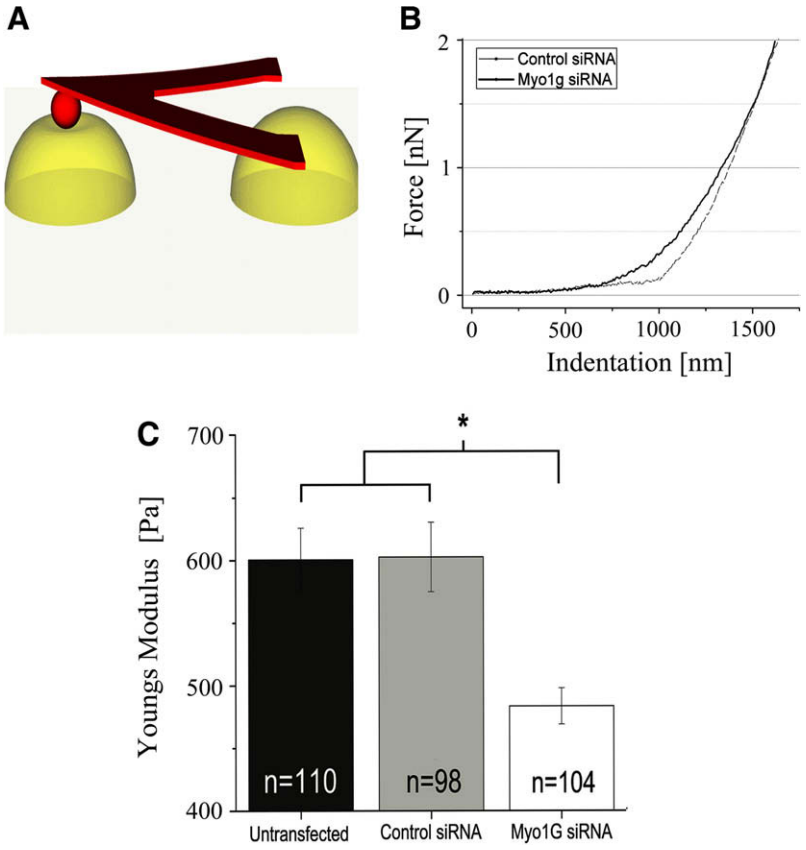

Fig. 5. Jurkat cells were transfected either with control siRNA or siRNA's targeting different regions of Myo1G mRNA using nucleofection. Seventy two hours post transfection Jurkat cells were used for elasticity measurement. (A) Schematic representation of indentation of Jurkat cells by a spherical glass bead mounted to an AFM cantilever. (B) Representative force–indentation curves of control siRNA and Myo1G siRNA treated cells. (C) Young's modulus (E) of untransfected, control siRNA and Myo1G siRNA treated cells. Mean ± SEM are given; $^{*}P < 0.01$, 'n' indicates the numbers of cells analysed.

as increasing the mass of the molecule to prevent its diffusion through the nuclear pores. Alternatively, the lack of the head domain might expose either a cryptic nuclear localization sequence or a specific nuclear binding site.

We found that the knockdown of Myo1G reduced the elasticity of Jurkat cells. The determined elasticity of 0.6 kPa for Jurkat cells is well within the range of values determined previously for Jurkat and other cells [26,12]. The knockdown of Myo1G most likely decreases cell elasticity by reducing internal tension on the actin cortex. We showed that Jurkat cells express in addition to Myo1G also Myo1b, Myo1c and Myo1e. The class I myosins Myo1a, Myo1b and Myo1c have been shown to act as force sensors. Their chemical ATPase cycle can be tuned by mechanical force [27–29]. The release of ADP is slowed significantly by load and as a consequence these class I myosins remain attached to F-actin for extended periods of time, because myosins in the ADP-bound state have a high affinity for F-actin. However, it is currently not known if Myo1G exhibits similar strain-sensitive motor properties. Unlike for the load-sensitive class I myosins, there was no additional small step noted upon ADP release in single molecule mechanical measurements for the most closely related class I myosin Myo1d [30]. Interestingly, overexpression of each of the mammalian myosins 1a, b, c, d and e caused an increase in membrane tension [15]. Therefore, it appears possible that the other class I myosins expressed in Jurkat cells also contribute to cell elasticity. However, they cannot compensate for the contribution of Myo1G. This is somewhat different from findings in *D. discoideum* cells. In these cells cortical tension was altered only when at least two different class I myosins were deleted simultaneously [14].

In conclusion, Myo1G participates in the regulation of cell elasticity in haematopoietic cells.

Acknowledgements

We thank Nino Zippelius for initial characterization of Myo1G antibodies and Myo1G localization studies. We thank Dr. Uwe Pieper for helpful discussions. We also thank Margrit Müller, Birgit Terstegge and Angelika Freitag for their technical assistance. This work was supported by the DFG (GRK 1050 and SFB 629).

References

[1] Nebl, T., Pestonjamasp, K.N., Leszyk, J.D., Crowley, J.L., Oh, S.W. and Luna, E.J. (2002) Proteomic analysis of a detergent-resistant membrane skeleton from neutrophil plasma membranes. J. Biol. Chem., 43399–43409.
[2] Hao, J.J., Wang, G., Pisitkun, T., Patino-Lopez, G., Nagashima, K., Knepper, M.A., Shen, R.F. and Shaw, S. (2008) Enrichment of distinct microfilament-associated and GTP-binding-proteins in membrane/microvilli fractions from lymphoid cells. J. Proteome Res., 2911–2927.
[3] Adams, R.J. and Pollard, T.D. (1989) Binding of myosin I to membrane lipids. Nature 340, 565–568.
[4] Hayden, S.M., Wolenski, J.S. and Mooseker, M.S. (1990) Binding of brush border myosin I to phospholipid vesicles. J. Cell Biol. 111, 443–451.
[5] Ruppert, C., Godel, J., Muller, R.T., Kroschewski, R., Reinhard, J. and Bähler, M. (1995) Localization of the rat myosin I molecules myr 1 and myr 2 and in vivo targeting of their tail domains. J. Cell Sci. 108, 3775–3786.
[6] Hokanson, D.E., Laakso, J.M., Lin, T., Sept, D. and Ostap, E.M. (2006) Myo1c binds phosphoinositides through a putative pleckstrin homology domain. Mol. Biol. Cell 17, 4856–4865.
[7] Brzeska, H., Hwang, K.J. and Korn, E.D. (2008) Acanthamoeba myosin IC colocalizes with phosphatidylinositol 4,5-bisphosphate at the plasma membrane due to the high concentration of negative charge. J. Biol. Chem. 283, 32014–32023.

[8] Coluccio, L.M. (2008) MyosinsProteins and Cell Regulation, pp. 95–124, Springer, Dordrecht, Netherlands.
[9] Huber, L.A., Fialka, I., Paiha, K., Hunziker, W., Sacks, D.B., Bähler, M., Way, M., Gagescu, R. and Gruenberg, J. (2000) Both calmodulin and the unconventional myosin Myr4 regulate membrane trafficking along the recycling pathway of MDCK cells. Traffic 1, 494–503.
[10] Spéder, P., Adám, G. and Noselli, S. (2006) Type ID unconventional myosin controls left–right asymmetry in *Drosophila*. Nature 440, 803–807.
[11] Hozumi, S., Maeda, R., Taniguchi, K., Kanai, M., Shirakabe, S., Sasamura, T., Spéder, P., Noselli, S., Aigaki, T., Murakami, R. and Matsuno, K. (2006) An unconventional myosin in Drosophila reverses the default handedness in visceral organs. Nature 440, 798–802.
[12] Janmey, P.A. and McCulloch, C.A. (2007) Cell mechanics: integrating cell responses to mechanical stimuli. Annu. Rev. Biomed. Eng. 9, 1–34.
[13] Gillespie, P.G. (2004) Myosin I and adaptation of mechanical transduction by the inner ear. Philos. Trans. R. Soc. Lond. B 359, 1945–1951.
[14] Dai, J., Ting-Beall, H.P., Hochmuth, R.M., Sheetz, M.P. and Titus, M.A. (1999) Myosin I contributes to the generation of resting cortical tension. Biophys. J. 77, 1168–1176.
[15] Nambiar, R., McConnell, R.E. and Tyska, M.J. (2009) Control of cell membrane tension by myosin-I. Proc. Natl. Acad. Sci. USA 106, 1972–1977.
[16] Stöffler, H.-E., Ruppert, C., Reinhard, J. and Bähler, M. (1995) A novel mammalian myosin I from rat with an SH3 domain localizes to Con A-inducible, F-actin-rich structures at cell–cell contacts. J. Cell Biol. 129 (3).
[17] Carl, P. and Schillers, H. (2008) Elasticity measurement of living cells with an atomic force microscope: data acquisition and processing. Pflugers Arch. 457, 551–559.
[18] Hutter, J.L. and Bechhoefer, J. (1993) Calibration of atomic-force microscope tips. Rev. Sci. Instrum. (USA) 64, 1868–1873.
[19] Sader, J.E. (2002) Calibration of atomic force microscope cantilevers in: Encyclopedia of Surface and Colloid Science (Hubbard, A., Ed.), pp. 846–856, Marcel Dekker, New York.
[20] Bejsovec, A. and Anderson, P. (1990) Functions of the myosin ATP and actin binding sites are required for *C. elegans* thick filament assembly. Cell 60, 133–140.
[21] Shimada, T., Sasaki, N., Ohkura, R. and Sutoh, K. (1997) Alanine scanning mutagenesis of the switch I region in the ATPase site of *Dictyostelium discoideum* myosin II. Biochemistry 36, 14037–14043.
[22] Weil, D., Levy, G., Sahly, I., Levi-Acobas, F., Blanchard, S., El-Amraoui, A., Crozet, F., Philippe, H., Abitbol, M. and Petit, C. (1995) Defective myosin VIIA gene responsible for Usher syndrome type IB. Nature 374, 60–61.
[23] Hokanson, D.E. and Ostap, E.M. (2006) Myo1c binds tightly and specifically to phosphatidylinositol 4,5-bisphosphate and inositol 1,4,5-trisphosphate. Proc. Natl. Acad. Sci. USA 103, 3118–3123.
[24] Bähler, M., Kroschewski, R., Stöffler, H.E. and Behrmann, T. (1994) Rat myr 4 defines a novel subclass of myosin I: identification, distribution, localization, and mapping of calmodulin-binding sites with differential calcium sensitivity. J. Cell Biol. 126, 375–389.
[25] Tang, N., Lin, T. and Ostap, E.M. (2002) Dynamics of myo1c (myosin-Ibeta) lipid biding and dissociation. J. Biol. Chem. 277, 42763–42768.
[26] Cai, X., Gao, S., Cai, J., Wu, Y. and Deng, H. (2009) Artesunate induced morphological and mechanical changes of Jurkat cell studied by AFM. Scanning 31 (83–89).
[27] Veigel, C., Coluccio, L.M., Jontes, J.D., Sparrow, J.C., Milligan, R.A. and Molloy, J.E. (1999) The motor protein myosin-I produces its working stroke in two steps. Nature 398, 530–533.
[28] Batters, C., Arthur, C.P., Lin, A., Porter, J., Geeves, M.A., Milligan, R.A., Molloy, J.E. and Coluccio, L.M. (2004) Myo1c is designed for the adaptation response in the inner ear. EMBO J. 23, 1433–1440.
[29] Laakso, J.M., Lewis, J.H., Shuman, H. and Ostap, E.M. (2008) Myosin I can act as a molecular force sensor. Science 321, 133–136.
[30] Köhler, D., Ruff, C., Meyhöfer, E. and Bähler, M. (2003) Different degrees of lever arm rotation control myosin step size. J. Cell Biol. 161 (Apr 28), 237–241.